2002

Ordered Clusters and Dynamical States of Particles in a Vibrated Fluid

G. A. Voth

B. Bigger

M. R. Buckley

Jerry P. Gollub
Haverford College

Ordered Clusters and Dynamical States of Particles in a Vibrated Fluid

Greg A. Voth,[1] B. Bigger,[1] M. R. Buckley,[1] W. Losert,[1,*] M. P. Brenner,[2] H. A. Stone,[2] and J. P. Gollub[1,3]

[1]*Department of Physics, Haverford College, Haverford, Pennsylvania 19041*

[2]*Division of Engineering and Applied Sciences, Harvard University, Cambridge Massachusetts 02138*

[3]*Department of Physics, University of Pennsylvania, Philadelphia, Pennsylvania 19104*

(Received 4 February 2002; published 20 May 2002)

Fluid-mediated interactions between particles in a vibrating fluid lead to both long range attraction and short range repulsion. The resulting patterns include hexagonally ordered microcrystallites, time-periodic structures, and chaotic fluctuating patterns with complex dynamics. A model based on streaming flow gives a good quantitative account of the attractive part of the interaction.

DOI: 10.1103/PhysRevLett.88.234301 PACS numbers: 45.70.Qj, 05.65.+b, 47.15.Cb, 47.55.Kf

Many important systems consist of granular material flowing while immersed in fluid. In early experiments, Bagnold used fluid saturated granular flows to remove the effects of gravity [1]. Others have avoided interstitial fluid (even removing air) in order to observe pure granular behavior. However, the fluid can produce interactions between particles resulting in interesting macroscopic effects. For example, granular heaping due to fluid interactions has been investigated in vertically vibrated deep granular beds [2,3]. A variety of interaction effects are also important in sedimentation and fluidized beds (for example, [4]).

In this Letter, we present experimental studies of novel phenomena that occur as a consequence of both attractive and repulsive interactions between non-Brownian particles when they are vibrated in a fluid. The observations include clustering, ordered crystalline patterns, and dynamical fluctuating states. The fluid mediated interactions can be tuned to produce a striking variety of dynamical phenomena. This provides an interesting new mechanism for self-assembly of ordered structures, complementary to other means of creating the interactions necessary for ordering [5–8].

The attractive interaction can be understood quantitatively using a theory based on the mean streaming flow generated by the oscillating particles. A short-range repulsive interaction is also observed at large vibrational acceleration. This repulsion shows a very sharp onset as the acceleration is increased. Together the combination of attraction and repulsion results in particles being bound together without contact over a range of parameters. We demonstrate how these interactions allow microcrystallites to form, for example hexagons surrounding a particle center. Small numbers of particles can form stable structures, while larger numbers of particles (>7) move chaotically in a bound state with no long range order, a "mesoscopic liquid."

The experimental setup is shown in Fig. 1. We conduct all experiments in a rigid 6 cm diameter by 1.5 cm tall cylindrical aluminum container vibrated vertically by an electromagnetic vibrator. We completely fill the container with a water/glycerol mixture of kinematic viscosity $\nu = 8$ cS (density $= 1.15$ gm/cm^3) and a submonolayer of uniform stainless steel spheres of radius $a = 0.397$ mm and density 8.0 gm/cm^3. A glass window seals the top of the cylinder to provide optical access and to avoid surface waves. The bottom plate is made of glass since its smoothness reduces random horizontal particle motion. We have used both flat glass and a concave lens for the bottom surface. The concave lens (focal length -1 m) makes no measurable change in the particle interactions; it is used to keep particles from slowly drifting to the edges of the cell due to imperfect leveling or slightly nonlinear vibrational motion.

Both the frequency ($\omega = 2\pi f$) and amplitude (S) of the vibration of the container are controlled externally. The nondimensional acceleration is given by $\Gamma = \omega^2 S/g$, where $g = 9.8$ m/s^2 is the acceleration of gravity. The container oscillations cause the particles to vibrate vertically, typically contacting the cell bottom once each cycle. The particles remain within three particle diameters from the bottom over the range of frequency and acceleration that we have explored. We image the entire system from above using a fast CCD camera. When the system is illuminated from an oblique angle, it is possible to measure the positions of the shadows of particles, and thereby to determine the amplitude of their vertical motion, A, defined as

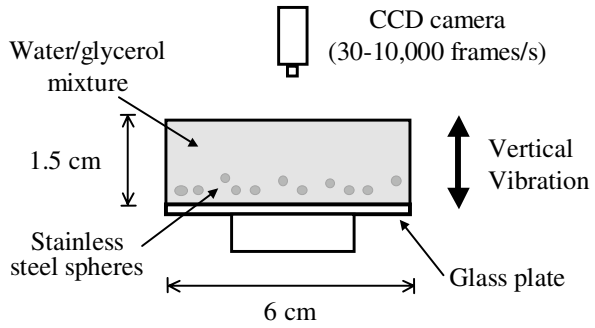

FIG. 1. Schematic of the apparatus in which particles are vibrated vertically in a viscous fluid. The vertical height of the cell is 19 times the particle diameter, so it approximates particles bouncing in a semi-infinite domain.

half the peak to peak displacement relative to the plate. The particle Reynolds number, $\mathrm{Re} = 2aA\omega/\nu$, ranges from 2 to 10.

In Fig. 2 we show the time evolution of an initially random distribution of particles. After the vibrator is started, the particles quickly collect into localized clusters, and the clusters then slowly coalesce in a manner reminiscent of coarsening in phase transitions.

A two particle system provides a particularly simple flow in which the particle attraction can be compared with theory. Figure 3 shows the distance between the centers of two particles as a function of time. The approach rate increases until they come into contact. The shape of these curves provides clear evidence that the clustering is due to a fluid-mediated interaction, and not to inelastic collisions, which cause clustering in a similar system with no fluid [9]. The separation also shows a small periodic modulation with the period of the vertical vibration. Particles separate near their lowest point and approach near the highest point of their motion.

The attractive interaction can be quantified by considering the flow produced by each individual particle's motion [10]. The vibrations produce an oscillatory flow around each particle, which is well approximated as a potential flow, outside of a boundary layer with approximate thickness $\delta_{\mathrm{osc}} = \sqrt{2\nu/\omega}$. In the experiment at $f = 50$ Hz, $\delta_{\mathrm{osc}} = 0.2$ mm, which is about half the particle radius. The potential flow near each oscillating particle is $\mathbf{u} = \nabla\phi$, where $\phi = -\frac{1}{2}A\omega\sin(\omega t)a^3\cos(\theta)/r^2$; here the origin is at the middle of the particle, and θ is the angle between a given location on the sphere and the forcing direction. At the particle surface, the component of the velocity field parallel to its surface is $u_{||}(\theta) = \frac{1}{2}A\omega \times \sin(\omega t)\sin(\theta)$ [11].

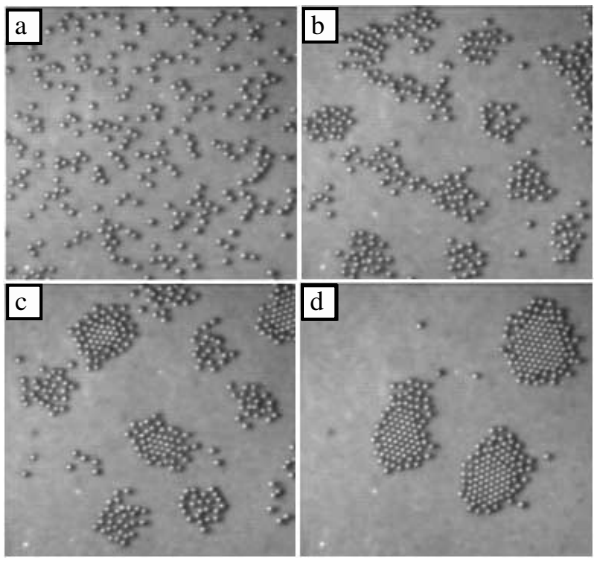

FIG. 2. Time evolution of an initially random distribution of beads. The attraction created by the streaming flow quickly collects the particles into clusters. ($f = 50$ Hz, $\Gamma = 4.5$) (a) $t = 0$ s; (b) $t = 8$ s; (c) $t = 16$ s; (d) $t = 32$ s.

Lord Rayleigh pointed out that when the magnitude of the oscillatory flow $u_{||} = u_{||}(\theta)$ varies along a solid surface, such as that of the particle, a *steady* secondary flow is generated [12,13]. For flow near the surface, mass conservation then requires that there is also a flow perpendicular to the boundary with magnitude $u_{\perp} \sim \delta_{\mathrm{osc}}\partial_{||}u_{||}$. Since this flow is not entirely out of phase with $u_{||}$ in the boundary layer, every oscillation cycle transports a finite amount of momentum into the boundary layer. Hence there is a time independent force density on the fluid in the boundary layer, which is parallel to the boundary and of order $\rho\langle u_{||}\partial_{||}u_{||}\rangle$, where ρ is the fluid density and $\langle\cdot\rangle$ denotes time average over a cycle. This forcing produces a steady flow, which when balanced against the viscous force $\rho\nu u_{\mathrm{steady}}/\delta_{\mathrm{osc}}^2$ gives the steady flow $u_{\mathrm{steady}} \sim -u_{||}\partial_{||}u_{||} \sim -A^2\omega/a\sin(\theta)\cos(\theta)$ at the edge of the oscillatory boundary layer.

This steady flow pushes fluid away from the poles of each particle [14]; and so there is a perpendicular inflow velocity towards the equator. This steady inflow is the origin of the attractive interactions between two particles.

The rate at which particles come together is determined by the steady inflow velocity far from the particle. Besides the oscillatory boundary layer, there is also a boundary layer caused by the steady flow itself [15], with a scale $\delta_{\mathrm{steady}} = a/\sqrt{\mathrm{Re}_{\mathrm{steady}}}$, where $\mathrm{Re}_{\mathrm{steady}} = A^2\omega/\nu$ is the Reynolds number of the steady secondary flow. The overall flow has been previously calculated numerically

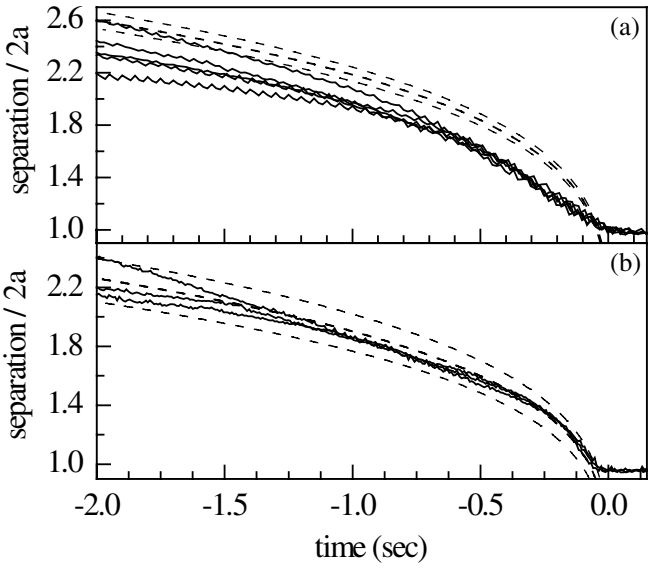

FIG. 3. Distance between two particles as they are brought together by the attractive flow. The solid curves are different experimental runs, and the central dashed curve shows the approach predicted by the steady streaming theory. Upper and lower dashed curves show the effect of measurement uncertainty in A. The time axes have been shifted so that the separation extrapolates to zero at $t = 0$. (a) $f = 20$ Hz, $\Gamma = 2.9$, $A = 0.41 \pm 0.04$ mm. Here the vertical particle motion is periodic. (b) $f = 50$ Hz, $\Gamma = 4.6$, $A = 0.15 \pm 0.04$ mm. The vertical motion is now chaotic and the mean oscillation amplitude is used for A in plotting the theoretical curve.

[14]. We find that an analytic matching argument, connecting the flows in the boundary layers to a potential flow far away, yields an explicit formula for the inflow velocity $v(r) = -0.53A\sqrt{\omega\nu}a^2/r^3$ at a distance r from the center of the sphere. Thus, if $R(t)$ denotes the distance between the particle centers, it follows that $dR/dt = 2v(R)$ since the particles follow the slow changes in the horizontal motion of the fluid. This implies that the separation between the two spheres should decrease according to the law

$$R(t) = (R_0^4 - 4.24A\sqrt{\omega\nu}a^2t)^{1/4}. \quad (1)$$

This formula assumes that (i) $\delta_{\text{osc}}/\delta_{\text{steady}} < 1$, which can be rewritten $A < a/\sqrt{2}$; (ii) the particles are far enough apart that they do not affect each other's boundary layers; and (iii) the influence of the bottom plate can be neglected. Our estimates indicate that assumption (i) holds when Γ is small or f is large, (ii) holds except at the final moments of approach, and (iii) holds except during the small interval in each cycle when the particle bounces off the plate.

In Fig. 3, the central dashed line shows the approach curves predicted by Eq. (1) for the conditions of the experiment. The agreement of the data with both the predicted functional form and rate of approach is quite good considering that all the parameters used by the theory are independently determined. At 20 Hz (Fig. 3a), the measured trajectories approach somewhat more slowly than the theory predicts. At 50 Hz (Fig. 3b), the measured approach rate is closer to the prediction, and the functional form agrees better, most likely because the oscillatory boundary layer is thinner in this case and so assumption (i) above is better satisfied. The upper and lower dashed curves show the effect of measurement uncertainty in A. Since at 50 Hz the amplitude is very small and the vertical motion is chaotic, the uncertainty is rather large in this case. Overall, the theory quite accurately captures the approach of two particles, and it seems unambiguous that the attraction is caused by the streaming mechanism.

At larger accelerations, a short-range repulsion becomes prominent and limits the closeness of approach. This can be seen in Fig. 4a, which displays the steady state separation between two particles as a function of Γ for forcing frequencies between 17 and 23 Hz. At each frequency, there is a steplike rise in separation at a characteristic Γ that moves to higher Γ as the frequency increases. The vertical motion of the particles remains periodic at these low frequencies, and Fig. 4b shows that there is no sharp change in the amplitude of the vertical motion with increasing Γ. From these observations we conclude that the onset of nonzero separation must be due solely to the fluid flow and not to changes in the bouncing dynamics. The onset of separation at each frequency appears when the particles have a peak-to-peak vertical amplitude of approximately 1.4 diameters.

A full explanation of this effect is not available. One possibility is that the repulsion becomes important when the oscillatory boundary layer is thicker than the steady boundary layer. An alternate explanation suggested by flow visualization is that the repulsion is due to recirculating zones near the particles created by deflection of the downward part of the streaming flow by the plate. Explaining the details of the repulsive interaction, particularly the sharp onset with acceleration, remains as a challenge for future work.

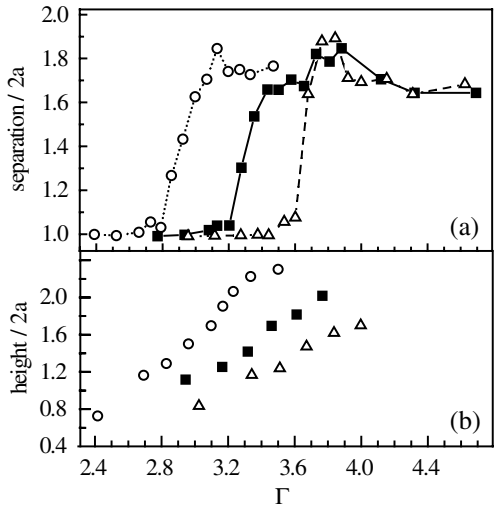

FIG. 4. (a) For two particles, the equilibrium distance between particle centers as a function of acceleration shows a rapid transition from contact to a nonzero separation. Separation is normalized by the particle diameter, $2a$. (b) Measurements of the peak to peak height (2A) that particles bounce above the plate show no dramatic change at the transition. Frequencies are 17 Hz (open circles), 20 Hz (filled squares), and 23 Hz (open triangles). Larger frequencies have the transition at larger acceleration.

Systems of more than two particles display a range of fascinating patterns and dynamics, including ordered crystallites, time-dependent ordered patterns, and bound states with complex particle motion. For example, one might expect that when attraction and repulsion are both important, the three particle system would form a stable symmetric triangular configuration. For low acceleration this is nearly the case, but, as the acceleration increases, the system breaks symmetry to a state with two paired and one distant particle as shown in Fig. 5(a). This state is fairly stable, but over long times the distant particle can wander close enough to cause a new pairing.

In a system with seven particles, stable hexagonal states form over the range $2.8 < \Gamma < 3.0$ (Fig. 5b). At slightly higher acceleration, the system switches to a time dependent state with two central particles rotating inside a ring of five others (Fig. 5c). Particle motion here is periodic and quite stable, a video animation of this "dance" is available online [16]. At yet higher acceleration, seven particle clusters exhibit apparently chaotic motion.

For larger numbers of particles, the presence of both attraction and repulsion leads to even more complex many-body effects, which are generally time dependent. Figures 5d–5f show a system of many particles at three different accelerations. Here the onset of a nonzero

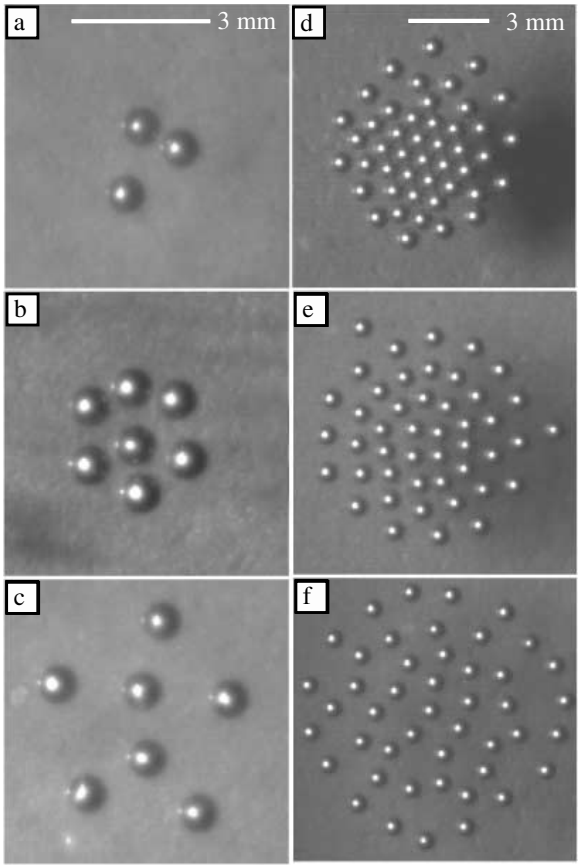

FIG. 5. Patterns formed by multiple particle systems when both attraction and repulsion are important. All images are acquired at $f = 20$ Hz. (a) Three particles at $\Gamma = 3.0$. (b) Seven particles in a stable hexagon at $\Gamma = 3.0$. (c) Seven particles in stable time-periodic motion at $\Gamma = 3.7$. (d) Many particles at $\Gamma = 3.7$, where the central particles are in contact and exterior particles are held apart by the hydrodynamic repulsion. (e) At $\Gamma = 3.9$ all the particles have separated and form a bound liquid. (f) $\Gamma = 5.3$, apparently chaotic. The time-dependent character of states (c) through (f) are revealed in on-line animations [16].

separation between particles occurs at higher acceleration than for the two particle case. As shown in Fig. 5(d) ($\Gamma = 3.7$), particles near the center of the cluster can remain in contact even when particles near the periphery have separated. One reason for this is that the vertical motion of particles is significantly smaller at the center of the cluster than at the edges, causing weaker repulsion. At $\Gamma = 3.9$, (Fig. 5e) the inner particles have separated and the system forms a bound state with weakly chaotic motion of all the particles, a mesoscopic liquid. One interesting feature of this state is that the preferred distance between particles results in the formation of closed shells. At the parameters of Fig. 5(e) there are two more particles than fit in the closed shells, and these "valence" particles move more freely than the others. Further increase of Γ results in increased interparticle distance and more rapid particle motion (Fig. 5f). Animations of these time-dependent states are available [16].

We emphasize that the apparently chaotic motion of particles in the clusters is not a result of external effects such as roughness of the driving surface. A single particle bounces regularly with possibly a slow drift, but many particles exhibit complicated motion. While a quantitative study remains for future work, it is natural to expect that the irregular motion is chaos resulting from the nonlinearity of the flow of the interstitial fluid.

In summary, we have shown that fluid mediated interactions between particles can be delicately tuned to produce a great variety of ordered and time-dependent dynamical states of these many-body systems.

This work has been supported in part by NSF Grants No. DMR-0079909 to Haverford College, No. DMR-0072203 to The University of Pennsylvania, and No. DMS-0296056 to Harvard University. We appreciate the hospitality of the Aspen Center for Physics, where this collaboration began. We also thank Arjun Yodh and Tom Lubensky for stimulating discussions on self-organization.

*Present address: IREAP, University of Maryland, College Park, Maryland 20742-3511.

[1] R. A. Bagnold, Proc. R. Soc. London A **225**, 49 (1954).
[2] H. K. Pak, E. Van Doorn, and R. P. Behringer, Phys. Rev. Lett. **74**, 4643 (1995).
[3] J. M. Schleier-Smith and H. A. Stone, Phys. Rev. Lett. **86**, 3016 (2001).
[4] A. F. Fortes, D. D. Joseph, and R. S. Lundgren, J. Fluid Mech. **177**, 467 (1987).
[5] M. Trau, D. A. Saville, and I. A. Aksay, Science **272**, 706 (1996).
[6] S. Yeh, M. Seul, and B. Shraiman, Nature (London) **386**, 57 (1997).
[7] T. Gong and T. W. M. Marr, Langmuir **17**, 2301 (2001).
[8] B. A. Grzybowski, H. A. Stone, and G. M. Whitesides, Nature (London) **405**, 1033 (1997).
[9] J. S. Olafsen and J. S. Urbach, Phys. Rev. Lett. **81**, 4369 (1998).
[10] G. K. Batchelor, *An Introduction to Fluid Dynamics,* (Cambridge University Press, Cambridge, 1967).
[11] The flow field around each particle is modified by the presence of the bottom boundary; within the potential flow approximation, having no mass flux across the plate requires an "image" particle beneath the plate, playing a similar role to image charges in electrostatics. Our estimates indicate that these image particles do not have a significant effect on the attractive interactions.
[12] Lord Rayleigh, Philos. Trans. R. Soc. London A **175**, 1 (1883).
[13] N. Riley, Annu. Rev. Fluid Mech. **33**, 43 (2001).
[14] N. Amin and N. Riley, J. Fluid Mech. **210**, 459 (1990).
[15] J. T. Stuart, J. Fluid Mech. **24**, 673 (1966).
[16] Video animations showing the time dependent states in Fig. 5 are available at (http://www.haverford.edu/physics-astro/gollub/clustering/). For archival purposes, they are also available as AIP Document No. EPAPS: E-PRLTAO-88-060222, which can be retrieved from the EPAPS homepage (http://www.aip.org/pubservs/epaps.html).